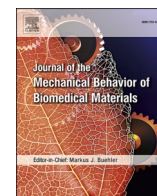




Contents lists available at ScienceDirect

Journal of the Mechanical Behavior of Biomedical Materials

journal homepage: <http://www.elsevier.com/locate/jmbbm>

The effect of different interference fits on the primary fixation of a cementless femoral component during experimental testing

Esther Sánchez^{a,*}, Christoph Schilling^b, Thomas M. Grupp^{b,c}, Alexander Giurea^d,
Caroline Wyers^{e,f}, Joop van den Bergh^{e,f,g}, Nico Verdonshot^{a,h}, Dennis Janssen^a

^a Radboud University Medical Center, Radboud Institute for Health Sciences, Orthopaedic Research Lab, Nijmegen, the Netherlands

^b Aesculap AG, Research & Development, Tuttlingen, Germany

^c Ludwig Maximilians University Munich, Department of Orthopaedic Surgery, Physical Medicine & Rehabilitation, Campus Grosshadern, Munich, Germany

^d Medical University of Vienna, Department of Orthopedics, Vienna, Austria

^e VieCuri Medical Center, Department of Internal Medicine, Venlo, the Netherlands

^f Maastricht University Medical Centre+ (MUMC+), Department of Internal Medicine, NUTRIM School of Nutrition and Translational Research in Metabolism, Maastricht, the Netherlands

^g Hasselt University, Biomedical Research Centre, Diepenbeek, Belgium

^h University of Twente, Laboratory for Biomechanical Engineering, Faculty of Engineering Technology, Enschede, the Netherlands

ARTICLE INFO

Keywords:

Interference fit
Cementless fixation
Micromotion
Interfacial gap
Digital image correlation
Bone deformation

ABSTRACT

Cementless femoral total knee arthroplasty (TKA) components use a press-fit (referred to as interference fit) to achieve initial fixation. A higher interference fit could lead to a superior fixation, but it could also introduce more damage to the bone during implantation. The purpose of the current study was to investigate the effect of interference fit on the micromotions and gap opening/closing at the bone-implant interface. Experimental tests were performed in six pairs of cadaveric femurs implanted with femoral components using a low interference fit of 350 μm and a high interference fit of 700 μm . The specimens were subjected to the peak loads of gait and squat, based on the Orthoload dataset. Digital Image Correlation (DIC) was used to measure the micromotions and opening/closing in different regions of interest (ROIs). Two linear mixed-effect statistical models were created with micromotions and gap opening/closing as dependent variables, ROIs, loading conditions, and implant designs as independent variables, and cadaver specimens as random intercepts. The results revealed no significant difference between the two interference fit implants for micromotions ($p = 0.837$ for gait and $p = 0.065$ for squat), nor for the gap opening/closing ($p = 0.748$ for gait and $p = 0.561$ for squat). In contrast, significant differences were found between loading and most of the ROIs in both dependent variables ($p < 0.0001$). Additionally, no difference in bone deformation was found between low and high interference fit. Changing interference between either 350 μm or 700 μm did not affect the primary stability of a femoral TKA component. There could be an interference fit threshold beyond which fixation does not further improve.

1. Introduction

Primary fixation of the implant to the bone is crucial for the long-term performance of total knee arthroplasty (TKA) (Chong et al., 2010), particularly in younger patients with a longer life expectancy (Kienapfel et al., 1999) and in older patients with low bone quality (Newman et al., 2017). For cementless implants, the primary fixation depends, amongst other parameters, on the press-fit provided by the implant system and on the frictional properties of the surface coating, which also allows for bone ingrowth on the long term (Campi et al.,

2018; Witmer and Meneghini, 2018; Damm et al., 2015). Primary stability is often expressed as the amount of relative displacement between the implant and the bone under physiological loads, referred to as micromotions (Abdul-Kadir et al., 2008; Tissakht et al., 1995). Animal studies have shown that if micromotions at the bone-implant interface are below 40 μm , bone will grow into the implant surface, while if micromotions are above 150 μm , a fibrous tissue formation will interfere with osseointegration and may eventually lead to aseptic loosening (Kienapfel et al., 1999; Abdul-Kadir et al., 2008; Reimeringer et al., 2013).

* Corresponding author. , Orthopaedic Research Lab 611, Geert Grooteplein Zuid 30, 6525, GA, Nijmegen, the Netherlands.

E-mail address: Esther.SanchezGarza@radboudumc.nl (E. Sánchez).

<https://doi.org/10.1016/j.jmbbm.2020.104189>

Received 6 March 2020; Received in revised form 30 September 2020; Accepted 26 October 2020

Available online 31 October 2020

1751-6161/© 2020 The Authors. Published by Elsevier Ltd. This is an open access article under the CC BY license (<http://creativecommons.org/licenses/by/4.0/>).

Press-fit fixation is achieved during surgery when the femoral component is impacted onto the bone, which is cut slightly larger than the internal dimensions of the implant. This size difference between implant and bone is called interference fit and is responsible for the compressive stresses acting at the bone-implant interface (Campi et al., 2018). Hence, in theory, a larger interference fit or higher press-fit should lead to higher compressive stresses that allow for higher frictional shear forces, and therefore, a superior fixation. However, these interface stresses can also cause some abrasion and permanent bone deformation during the insertion of the implant (Damm et al., 2015; Abdul-Kadir et al., 2008), which negatively influences the press-fit. This permanent bone deformation is found predominantly in the anterior flange and the posterior condyles (Fig. 1), due to the clamping mechanism of femoral press-fit implants (Berahmani et al., 2018).

Ideally, full contact between the implant and the bone is achieved during surgery to facilitate long-term fixation through osseointegration. However, the bone cuts do not always match the implant, which creates gaps between the implant and the bone (Pettersen et al., 2009). Although bone ingrowth is possible even for interface gaps of 1–2 mm (Goodman et al., 2013), these gaps may open and close during physiological loading and may influence primary and secondary fixation.

The most optimal interference fit of femoral TKA components is still unclear. A better understanding of micromotions at the bone-implant interface, and the effect of surface morphology, interference fit, bone damage, and loading conditions thereon, could provide more information about the mechanism of fixation of cementless femoral implants. The objective of the current study was therefore to investigate the effect of interference fit on micromotions and gap opening/closing occurring at the bone-implant interface of a femoral TKA component during experimental testing.

2. Material and methods

2.1. Specimen preparation

Six pairs of fresh-frozen human cadaveric femurs (average age 55) were used in this study (Table 1). After dissection, an experienced orthopedic surgeon (AG) prepared the femur cuts following the surgical guidelines (Aesculap AG, Tuttlingen, Germany) thereby taking into account that the nominal cuts of the bones fit perfectly to the internal surface of the implants before coating. Next, the specimens were scanned with a high resolution peripheral quantitative computed tomography (HR-pQCT - Xtreme CT II, SCANCO Medical AG, Brüttisellen, Switzerland) at a resolution of 61 μm . After all femurs had been scanned, they were implanted with two cementless e.motion® femoral components (e.motion® Knee System; Aesculap Tuttlingen, Germany) with different coating thickness (sizes are provided in Table 1). Low interference fit implants with a thickness of 350 μm and Plasmapore® coating were used for the right femurs, while high interference fit implants with a thickness of 700 μm and a similar surface coating were placed in the left femurs.

After implantation, the femurs were cut proximally and cast in bone

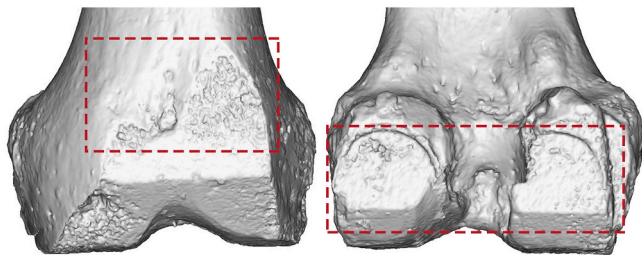


Fig. 1. HR-pQCT images of cadaver specimens after removing implants, the rectangles show an implant imprint in the anterior flange and in the posterior condyles.

Table 1

Specimen details for age, Body Mass Index (BMI), sex, implant size, and loading forces for gait and squat. The last row shows the average \pm SD of age and BMI of the cadaver bone donors.

Specimen number	Age	BMI	Sex	Implant size	Load Gait (N)	Load 50% Squat (N)
1	57	28.74	M	7	2718	1342
2	60	23.4	F	5	1725	852
3	60	30.38	F	5	2300	1136
4	59	30.89	F	4	2143	1058
5	47	28.49	F	5	1960	968
6	50	36.31	F	4	2430	1200
	55	30 \pm				
	\pm 5	4				

cement (PMMA). Subsequently, a speckle pattern was applied using black and white spray paint following a previous experimental protocol (Berahmani et al., 2017) to facilitate Digital Image Correlation (DIC) measurements. The specimens were thawed at room temperature for 3 h before applying the speckle pattern and allowed to dry for 16 h before performing the experiments.

2.2. Surface morphology

The high interference fit implants were generated by taking the low interference fit implants out of the manufacturing process just before being coated. The thicker coating was then applied to these implants at a medical coating manufacturer (DOT GmbH, Rostock, Germany). The coating characteristics were determined using confocal microscopy to assess the resemblance with low interference fit coating. Although both coatings were applied to the femoral components using similar manufacturing process, small differences in grain size were observed with the low interference fit having a finer grain morphology coating compared to the high interference fit (Fig. 2). In addition, a slightly lower roughness value was found for the low interference fit coating as compared to the high interference fit coating with Ra of 41.51 \pm 0.99 μm and 52.21 \pm 6.83 μm , respectively.

2.3. Loading conditions

Mechanical experiments were performed in an MTS machine (MTS Systems Corporation, Eden Prairie, Minnesota, USA) using a custom-made load applicator that integrated the tibial component and insert (Fig. 3A). First, specimens underwent a preconditioning loading regime for 15 min at 1 Hz using the same forces as used for the micromotions measurements (Table 1). The peak loads of gait and squat were applied to the reconstructions based on the Orthoload database (Average 75 - Bergmann, 2008) and adjusted to the cadaver donors bodyweight (BW). After a resting period of 15 min, the full-scale load was applied at 100N/s. For squat loading, only 50% of the maximum load was applied to prevent distal fractures of the femurs at the PMMA fixation base (Berahmani et al., 2017).

Varus-valgus moments reported in the Orthoload database were incorporated by offsetting the axial force medially at 9 mm for gait, and 3.6 mm for squat (Halder et al., 2012; Kutzner et al., 2017) Furthermore, the specimens were fixed distally at 14 degrees of flexion (gait) and 90° (squat), coinciding with the flexion angles at peak load (Bergmann, 2008).

2.4. Micromotion measurements

Micromotions at the implant-bone interface were measured using DIC at different regions of interest (ROIs) during three repetitions. For gait, 9 ROIs were defined: anterior flange (ANT); anterior, distal, and posterior region of the medial (MA, MD, MP) and lateral (LA, LD, LP) views; and the medial and lateral posterior condyles (CM, CL). For squat,

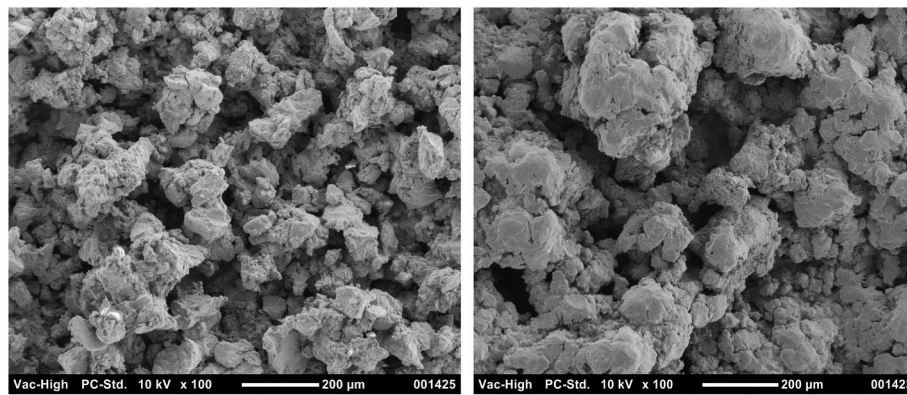


Fig. 2. Scanning electron microscopy images (SEM, NeoScope JCM-5000) of the low interference fit coating (left) and high interference fit (right).

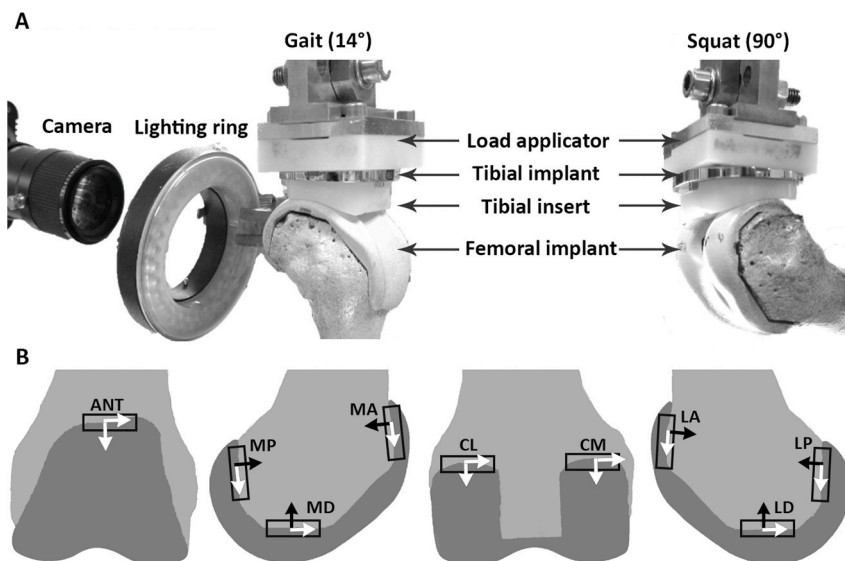


Fig. 3. A) Experimental setup for gait loading at 14° and squat loading at 90°. B) The 9 Regions of interest (ROIs) for gait defined at the bone-implant interface for the anterior flange (ANT); the anterior, distal, and posterior region of the medial (MA, MD, MP) and lateral (LA, LD, LP) views; and the lateral and medial condyles (CL, CM). For squat, the anterior flange and the condyles were not measured, so there are 6 ROIs. Micromotions are parallel to the interface (white arrows), and gap opening/closing perpendicular (black arrows).

only 6 ROIs were included, as measurements were not possible in the posterior condyles and the anterior flange (Fig. 3A). A first image was taken without loading and a second image after loading, then the relative displacements induced by the loading regime were determined by comparing the “loaded” with the “unloaded” images.

The shear and normal components of the displacement were calculated using DIC software (GOM Correlate, Freeware, 2017. GOM Inc., Braunschweig, Germany) by defining a local coordinate system based on the orientation of the interface in the image. Micromotions were defined as the shear component, while opening and closing of the interface were defined as the normal component of displacement (Fig. 3B).

2.5. Quantification of permanent bone deformation

The implants were cut through the distal condyles to remove these without further damaging the bone. Afterwards, the femurs were scanned again using HR-pQCT (Xtreme CT II, SCANCO Medical AG, Brüttlingen, Switzerland). The images were converted to surface meshes (Mimics 20, Materialise, Leuven, Belgium) and remeshed (3-Matic 12, Materialise, Leuven, Belgium). The pre- and post-implantation surface meshes were then registered onto each other at the bone surfaces outside of the interface region using coherent point drift (CPD) and iterative closest point (ICP) algorithms. These surface registrations were compared to quantify the permanent deformation on the exterior of the bone generated during implantation and subsequent loading, which was referred to as damage in this paper.

2.6. Statistical analysis

Two multilevel linear mixed-effect models were created in STATA (Release 15. College Station, TX: StataCorp LLC) for the dependent variables of micromotions and gap opening/closing during gait and squat loading. Design (low and high interference fit), loading conditions, and the ROIs were the independent variables, while cadaver specimens were considered as the random intercepts. For micromotion results, a log-transformation was performed to meet normality, but this was not necessary for opening and closing results. Moreover, a pairwise comparison was made for all the ROIs. A p-value < 0.05 was considered as statistical significant.

3. Results

3.1. Interface micromotions

Statistical analysis of the micromotions in the multilevel models revealed no significant difference between low and high interference fit implants ($p = 0.837$ for gait and $p = 0.065$ for squat). The mean micromotions are summarized in Table 2. During gait, the largest micromotions (Fig. 4) were found in the posterior condyles (CM, MP), followed by the medial anterior region (MA). For squat, the largest micromotions were seen in the distal regions (LD, MD). The ROIs with no significant difference were MD, LD, LP for gait and MP, LP, MA for squat.

Table 2

Results for mean micromotions and mean gap opening/closing with 95% confidence interval (CI) for both interference fits during gait and squat.

Interference fit	LOADING CONDITIONS	MEAN MICROMOTIONS (μm)	95% CI (μm)		MEAN OPENING/CLOSING (μm)	95% CI (μm)	
Low	Gait	25	18	32	-17	-27	-6
	Squat	28	20	37	14	-1	30
High	Gait	30	20	40	-16	-29	-3
	Squat	31	23	40	14	0	28

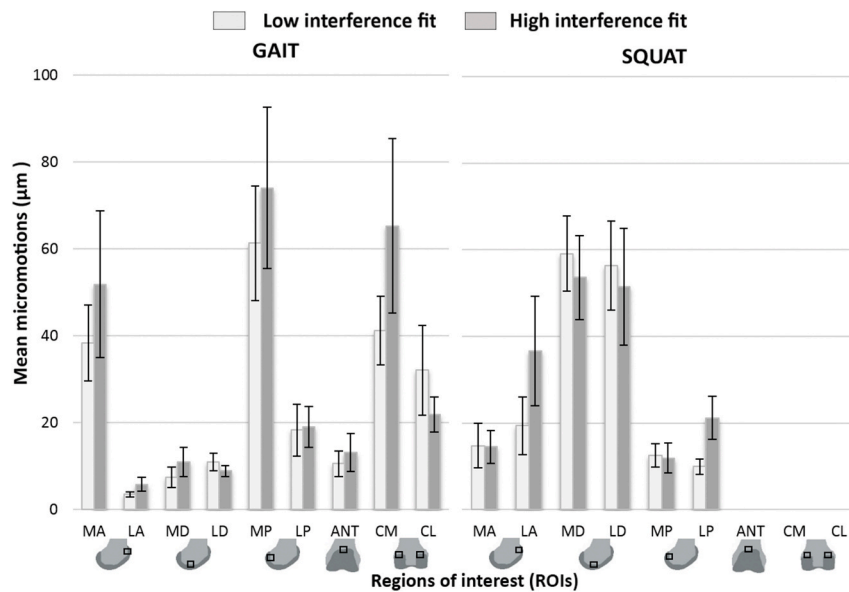


Fig. 4. Mean micromotions with standard error of mean at the ROIs (MA: medial anterior; LA: lateral anterior; MD: medial distal; LD: lateral distal; MP: medial posterior; LP: lateral posterior; ANT: anterior flange; CM: medial condyle CL: lateral condyle) of low and high interference fit implants. During squat, measurements were not possible in the anterior and posterior condyles.

3.2. Interfacial gaps

Similar to the findings for the micromotions, no significant difference was found between implant interference fits for the gaps results ($p = 0.748$ for gait and $p = 0.561$ for squat). The positive values indicated a gap opening, whereas the negative values a gap closing. The mean opening and closing are presented in Table 2. During gait (Fig. 5), gap opening is negligible and gap closing is noticed mainly in the distal

regions (MD, LD). In contrast, for squat there is gap opening in the anterior regions (MA, LA), and gap closing in the posterior regions (MP, LP). No significant differences were found in the ROIs LP, MA, MP for gait and MA for squat.

3.3. Permanent bone deformation

After removal of the implants from the femurs, visual inspection of

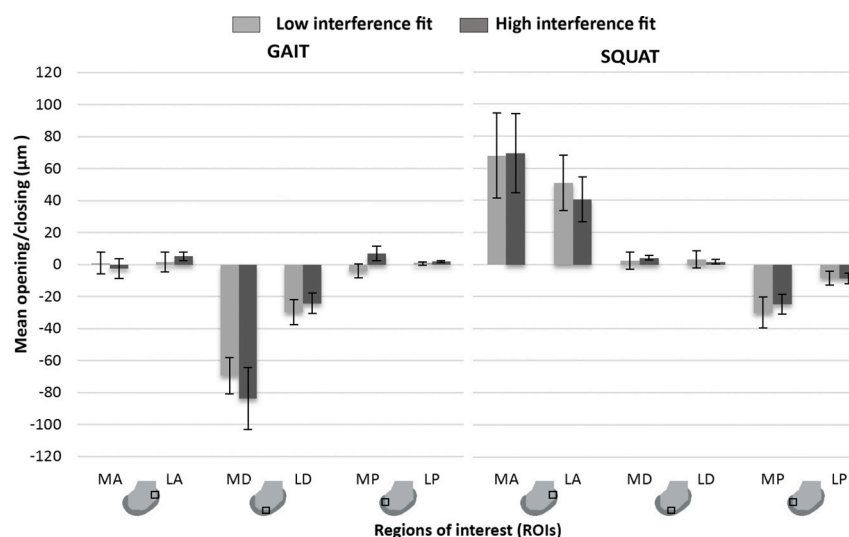


Fig. 5. Mean opening (positive) and closing (negative) with a standard error of mean at the ROIs (MA: medial anterior; LA: lateral anterior; MD: medial distal; LD: lateral distal; MP: medial posterior; LP: lateral posterior) of low and high interference fit implants.

the specimens did not show a clear distinction between the imprints that the low and high interference fit implants had made on the bone. While in some cases, the high interference fit revealed more bone compression than the low interference fit, in other cases the effect was reversed. For example, in Fig. 6, the specimen 1-High interference fit had more damage around the condyles than the 1-Low interference fit, whereas specimen 3-Low interference fit had more damage than the 3-High interference fit.

The results of the HR-pQCT registration, represented in distribution plots (Figs. 7 and 8) quantify the permanent deformation seen after implant removal with negative values indicating bone compression; the positive values were neglected to focus on the damage on the anterior and posterior regions. The posterior condyles displayed more damage and nearly all specimens had an implant imprint, except specimens 4 and 6 for the low interference fit implants. Overall, almost no difference in damage was found between the implant designs.

4. Discussion

The goal of this study was to assess the effect of interference fit on primary stability between two cementless femoral TKA components. In our study we found no significant difference in stability between the two interference fits.

The lack of difference between micromotions of low and high interference fit implants could be attributed to the amount of damage that is introduced to the bone during the insertion of the implant. Permanent bone deformation was mainly found in the condyles and anterior flange, which is similar as reported by another study (Berahmani et al., 2018). However, in our study, there was almost no difference in bone damage seen between the two implants. Bone damage was quantified through a surface registration of HR-pQCT scans made before and after implantation. Although the resolution of the HR-pQCT scans (61 μm) should be sufficient to pick up a 350 μm difference in an interference fit, perhaps another approach for deformation measurements that involves volumetric-based registration, such as used in digital volume correlation (Rapagna et al., 2019), may provide more insight into the actual damage profiles, and the effect of interference fit.

The loading configuration had a significant effect on both dependent variables (micromotions and opening/closing). During gait, the load was applied to the distal condyles, which is where the most gap closing was measured (MD and LD). Under the same loading configuration, the largest micromotions were seen in the anterior and posterior ROIs (MP, MA, CM, CL), where the force was aimed parallel to the bone-implant

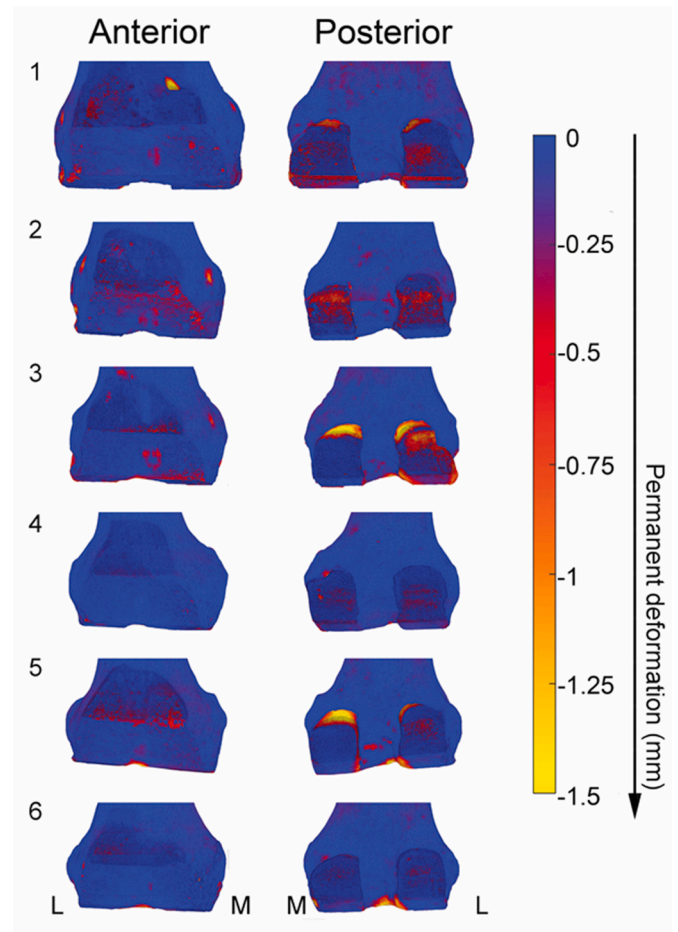


Fig. 7. Permanent bone deformation after implant removal shown at the anterior flange (left) and posterior condyles (right) for the low interference fit implants. The distribution plots give a quantification of the amount of bone damage.

interface. Conversely, during squat, the force was applied to the posterior condyles, so closing was mainly seen in the posterior ROIs (MP, LP), while opening was seen in the anterior ROIs (MA, LA), as the forces were aimed perpendicular to these interfaces. Similarly, the largest

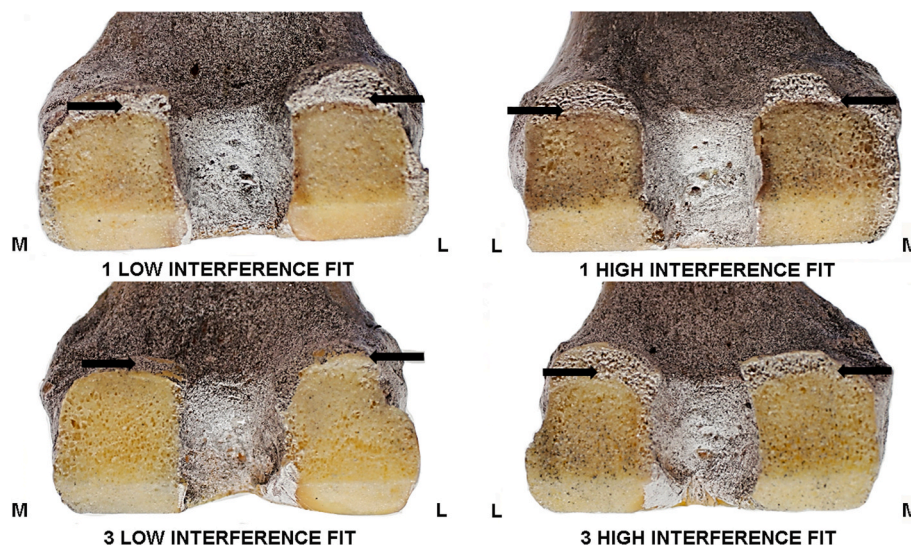


Fig. 6. Posterior regions of bone specimens after removing implants, the arrows show the edges of the implant imprint into the bone.

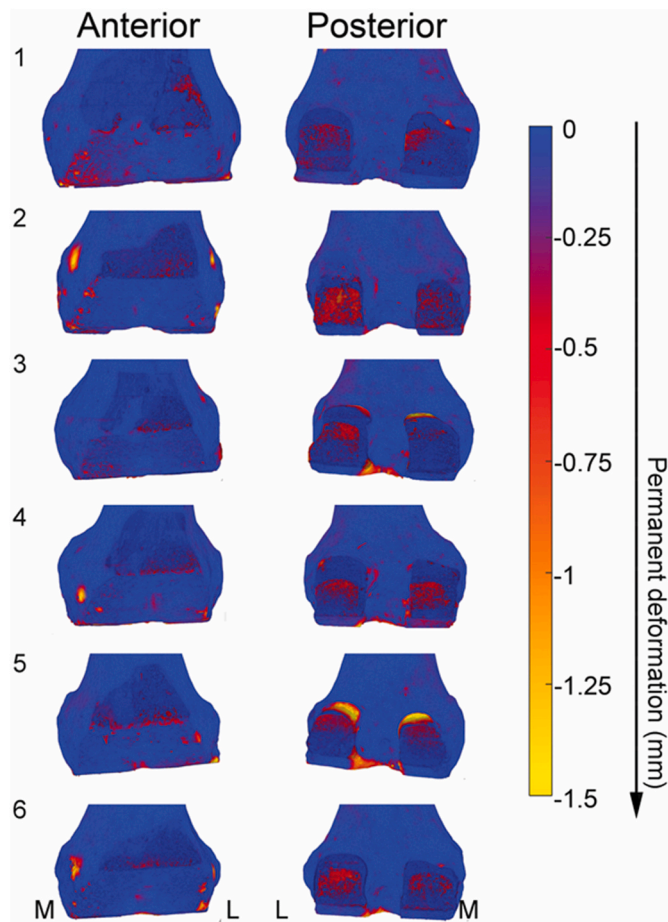


Fig. 8. Permanent bone deformation after implant removal shown at the anterior flange (left) and posterior condyles (right) for the high interference fit implants. The distribution plots give a quantification of the amount of bone damage.

micromotions were found in the interfaces parallel to the load vector, in the distal ROIs (MD, LD). We also saw differences between the medial and lateral ROIs, due to the medial distribution of the load. Our results are comparable to [Berahmani et al. \(2017\)](#), the small differences in micromotions may be attributed to the loading regime, implant designs, coating thickness, and bone quality.

Our experimental results of micromotions and interfacial gaps of the e.motion® implant are below the threshold of good primary stability. This is in agreement with clinical results from cementless e.motion® femoral component with an interference fit of 350 μm , where there was a survival rate of 100% at 5.6 years postoperatively in TKA hybrid implants ([Chavoix, 2013](#)). In addition, another study showed a survival rate of 96.2% for cementless TKA components and 96.3% for hybrid TKA components after 8.3 years postoperatively ([Lass et al., 2013](#)). Currently, the standard e.motion® Knee System is designed with an interference fit of 350 μm . Based on the results of the current study, it can be expected that allowing for manufacture tolerances or increasing the interference fit to 700 μm still provides a good initial fixation.

4.1. Limitations

In order to be able to load the implant-bone interface, some concessions had to be made to the loading configuration. Firstly, we had to reduce the load to 50% to avoid the fracture risk during the squat load. Secondly, rather than applying a full loading cycle, we were only able to apply the peak forces of gait and squat. Thirdly, only the axial force from Orthoload was considered, ignoring the shear forces that may cause

larger micromotions ([Chong et al., 2010](#)), and the patellar forces that can stabilize the force to the femoral condyles ([Berahmani et al., 2016](#)). Finally, it was only possible to measure the micromotions outside of the bone-implant interface. Nevertheless, this study could be used to validate FE models of implant-bone interface mechanics, which in turn could evaluate the effect of full loading cycles and all the forces involved in this type of activities directly at the bone-implant interface.

Femur preparation was performed using standard surgical instruments, mimicking the clinical situation as closely as possible. One limitation related to this choice is the cutting errors that may have occurred. Unfortunately, due to the angular difference between the cutting planes, the differences between the condyles, and the variation in implant size, we were unable to determine a reproducible reference point for the quantification of bone cuts that could be subtracted from the theoretical interference fit. However, in a previous study with a different femoral component ([Berahmani et al., 2017](#)), the cutting errors were measured using a 3D optical scanner (ATOS 3D-scanner, GOM GmbH, Braunschweig, Germany). That study reported cutting errors of 80–170 μm in the AP direction (dependent on the implant system). While these errors are 2–4 times smaller than the difference in interference fit that was studied here, they may still have influenced the primary fixation.

Other limitations in our study were the conditions used in our laboratory, which were different from a real TKA surgical procedure. To be able to make the HR-pQCT scans, it was necessary first to make the bone cuts, then the implantation of the femoral components. Thus the re-freezing cycles of the bones could have affected their properties. Besides, there may be differences in bone quality between the bone specimens, and some deviation between bone cuts on the right and left knee or implant position. However, these forms of variability should be considered to robustly evaluate the primary fixation of press-fit components.

These limitations do not reduce the validity of our study since few studies have reported on femoral micromotions, and most of these used linear variable differential transducers (LVDTs) ([Conlisk et al., 2018](#); [Cristofolini et al., 2008](#)). However, LVDTs measure micromotions at a certain distance from the bone-implant interface, and therefore can also introduce a fraction of bone deformation into the measurements ([Gortchacow et al., 2012](#)). In addition, to our knowledge, we are the first study to include the normal micromotions results and quantify the difference in gap opening and closing.

4.2. Conclusion

Experimental tests were performed on cementless femoral implants with two different interference fits to investigate the primary stability using micromotions and gap opening. The results did not demonstrate significant differences between the designs. Moreover, the bone deformation results do not show a distinction between low and high interference fit implants. Nevertheless, the results for micromotions and gap opening, as obtained in this study, indicate that the implants with high interference fit are likely to perform as good as the low interference fit implants during the immediate postoperatively situation.

CRediT authorship contribution statement

Esther Sánchez: Conceptualization, Methodology, Software, Validation, Formal analysis, Investigation, Writing - original draft, Visualization, Project administration. **Christoph Schilling:** Conceptualization, Resources, Writing - review & editing, Supervision, Funding acquisition. **Thomas M. Grupp:** Conceptualization, Resources, Writing - review & editing, Supervision, Funding acquisition. **Alexander Giurea:** Resources, Writing - review & editing. **Caroline Wyers:** Resources, Writing - review & editing. **Joop van den Bergh:** Resources, Writing - review & editing. **Nico Verdonshot:** Conceptualization, Methodology, Validation, Resources, Writing - review & editing, Supervision. **Dennis**

Janssen: Conceptualization, Methodology, Validation, Resources, Writing - review & editing, Supervision, Project administration.

Declaration of competing interest

The authors declare that they have no known competing financial interests or personal relationships that could have appeared to influence the work reported in this paper.

Acknowledgements

A research grant from Aesculap (Aesculap, B. Braun, Tuttlingen, Germany) supported this work. We would like to thank Dr. Thomas Hoogbeem for his help in developing the statistical model, Richard van Swam for the help and support during the experimental tests, Léon Driessen for all the segmentation work with the HR-pQCT scans, Max Bakker for the Matlab support, and Erik de Vries for the surface morphology measurements. We are also thankful to Justine Eerden for her collaboration in this project.

References

- Abdul-Kadir, M.R., Hansen, U., Klabunde, R., Lucas, D., Amis, A., 2008. Finite element modelling of primary hip stem stability: the effect of interference fit. *J. Biomech.* 41, 587–594. <https://doi.org/10.1016/j.jbiomech.2007.10.009>.
- Berahmani, S., Hendriks, M., de Jong, J.J.A., van den Bergh, J.P.W., Maal, T., Janssen, D., Verdonchot, N., 2018. Evaluation of interference fit and bone damage of an uncemented femoral knee implant. *Clin. Biomech.* 51, 1–9. <https://doi.org/10.1016/j.clinbiomech.2017.10.022>.
- Berahmani, S., Hendriks, M., Wolfson, D., Wright, A., Janssen, D., Verdonchot, N., 2017. Experimental pre-clinical assessment of the primary stability of two cementless femoral knee components. *J. Mech. Behav. Biomed. Mater.* 75, 322–329. <https://doi.org/10.1016/j.jmbbm.2017.07.043>.
- Berahmani, S., Janssen, D., Wolfson, D., De Waal Malefijt, M., Fitzpatrick, C.K., Rullkoetter, P.J., Verdonchot, N., 2016. FE analysis of the effects of simplifications in experimental testing on micromotions of uncemented femoral knee implants. *J. Orthop. Res.* 34, 812–819. <https://doi.org/10.1002/jor.23074>.
- Bergmann, G., 2008. Orthoload [WWW Document]. Charité Univ, Berlin.
- Campi, S., Mellon, S.J., Ridley, D., Foulke, B., Dodd, C.A.F., Pandit, H.G., Murray, D.W., 2018. Optimal interference of the tibial component of the cementless oxford unicompartmental knee replacement. *Bone Joint Res* 7, 226–231. <https://doi.org/10.1302/2046-3758.73.BJR-2017-0193.R1>.
- Chavoix, J.-B., 2013. Functionality and Safety of an Ultra-Congruent Rotating Platform Knee Prosthesis at 5.6 Years: more than 5- Year Follow-Up of the e.motion ((®)) UC-TKA. *Open Orthop. J.* 7, 152–157. <https://doi.org/10.2174/1874325001307010152>.
- Chong, D.Y.R., Hansen, U.N., Amis, A.A., 2010. Analysis of bone-prosthesis interface micromotion for cementless tibial prosthesis fixation and the influence of loading conditions. *J. Biomech.* 43, 1074–1080. <https://doi.org/10.1016/j.jbiomech.2009.12.006>.
- Conlisk, N., Howie, C.R., Pankaj, P., 2018. Quantification of interfacial motions following primary and revision total knee Arthroplasty : a verification study versus experimental data. *J. Orthop. Res.* 36, 387–396. <https://doi.org/10.1002/jor.23653>.
- Cristofolini, L., Affatato, S., Erani, P., Leardini, W., Tigani, D., Viceconti, M., 2008. Long-term implant-bone fixation of the femoral component in total knee replacement. *Proc. Inst. Mech. Eng. Part H J. Eng. Med.* 222, 319–331. <https://doi.org/10.1243/09544119JEM328>.
- Damm, N.B., Morlock, M.M., Bishop, N.E., 2015. Friction coefficient and effective interference at the implant-bone interface. *J. Biomech.* 48, 3517–3521. <https://doi.org/10.1016/j.jbiomech.2015.07.012>.
- Goodman, S.B., Yao, Z., Keeney, M., Yang, F., 2013. The future of biologic coatings for orthopaedic implants. *Biomaterials* 34, 3174–3183. <https://doi.org/10.1016/j.biomaterials.2013.01.074>.
- Gortchacow, M., Wettstein, M., Pioletti, D.P., Müller-Gerbl, M., Terrier, A., 2012. Simultaneous and multisite measure of micromotion, subsidence and gap to evaluate femoral stem stability. *J. Biomech.* 45, 1232–1238. <https://doi.org/10.1016/j.jbiomech.2012.01.040>.
- Halder, A., Kutzner, I., Graichen, F., Heinlein, B., Beier, A., Bergmann, G., 2012. Influence of limb alignment on mediolateral loading in total knee replacement. *J. Bone Jt. Surgery-American* 94, 1023–1029. <https://doi.org/10.2106/JBJS.K.00927>.
- Kienapfel, H., Sprey, C., Wilke, A., Griss, R., 1999. Implant fixation by bone ingrowth. *J. Arthroplasty* 14, 355–368 (99)90063-3. <https://doi.org/10.1016/S0883-5403>.
- Kutzner, I., Bender, A., Dymke, J., Duda, G., Von Roth, P., Bergmann, G., 2017. Mediolateral force distribution at the knee joint shifts across activities and is driven by tibiofemoral alignment. *Bone Jt. J.* 99B, 779–787. <https://doi.org/10.1302/0301-620X.99B6.BJJ-2016-0713.R1>.
- Lass, R., Kubista, B., Holinka, J., Pfeiffer, M., Schuller, S., Stenicka, S., Windhager, R., Giurea, A., 2013. Comparison of cementless and hybrid cemented total knee arthroplasty. *Orthopedics* 36, e420–e427. <https://doi.org/10.3928/01477447-20130327-16>.
- Newman, J.M., Khlopas, A., Chughtai, M., Gwam, C.U., Mistry, J.B., Yakubek, G.A., Harwin, S.F., Mont, M.A., 2017. Cementless total knee arthroplasty in patients older than 75 years. *J. Knee Surg.* 30, 930–935. <http://goi.org/10.1055/s-0037-1599253>.
- Petersen, S.H., Wik, T.S., Skallerud, B., 2009. Subject specific finite element analysis of implant stability for a cementless femoral stem. *Clin. Biomech.* 24, 480–487. <https://doi.org/10.1016/j.clinbiomech.2009.03.009>.
- Rapagna, S., Berahmani, S., Wyers, C.E., van den Bergh, J.P.W., Reynolds, K.J., Tozzi, G., Janssen, D., Perilli, E., 2019. Quantification of human bone microarchitecture damage in press-fit femoral knee implantation using HR-pQCT and digital volume correlation. *J. Mech. Behav. Biomed. Mater.* 97, 278–287. <https://doi.org/10.1016/j.jmbbm.2019.04.054>.
- Reimeringer, M., Nuño, N., Desmarais-Trépanier, C., Lavigne, M., Vendittoli, P.A., 2013. The influence of uncemented femoral stem length and design on its primary stability: a finite element analysis. *Comput. Methods Biomech. Biomed. Eng.* 16, 1221–1231. <https://doi.org/10.1080/10255842.2012.662677>.
- Tissakht, M., Eskandari, H., Ahmed, A.M., 1995. Micromotion analysis of the fixation of total knee tibial component. *Comput. Struct.* 56, 365–375. [https://doi.org/10.1016/0045-7949\(95\)00029-G](https://doi.org/10.1016/0045-7949(95)00029-G).
- Witmer, D.K., Meneghini, R.M., 2018. Cementless total knee arthroplasty: patient selection and surgical techniques to optimize outcomes. *Semin. Arthroplasty* 29, 50–54. <https://doi.org/10.1053/j.sart.2018.04.003>.